JOC The Journal of Organic Chemistry

Article

pubs.acs.org/joc

Effect of a Bromo Substituent on the Glutathione Peroxidase Activity of a Pyridoxine-like Diselenide

Vijay P. Singh,*[,†] Jia-fei Poon,[†] Ray J. Butcher,[‡] Xi Lu,[§] Gemma Mestres,[§] Marjam Karlsson Ott,[§] and Lars Engman*[,†]

[†]Department of Chemistry−BMC, Uppsala University, Box 576, SE-751 23 Uppsala, Sweden

[‡]Department of Chemistry, Howard University, Washington, D.C. 20059, United States

[§]Division of Applied Materials Science, Department of Engineering Sciences, Uppsala University, SE-751 23 Uppsala, Sweden

Supporting Information

ABSTRACT: In search for better mimics of the glutathione peroxidase enzymes, pyridoxine-like diselenides **6** and **11**, carrying a 6-bromo substituent, were prepared. Reaction of 2,6-dibromo-3-pyridinol **5** with sodium diselenide provided **6** via aromatic nucleophilic substitution of the 2-bromo substituent. $LiAlH_4$ caused reduction of all four ester groups and returned **11** after acidic workup. The X-ray structure of **6** showed that the dipyridyl diselenide moiety was kept in an almost planar, transoid conformation. According to NBO-analysis, this was due to weak intramolecular Se···O (1.1 kcal/mol) and Se···N-interactions (2.5 kcal/mol). That the 6-bromo substituent increased the positive charge on selenium was confirmed by NPA-analysis and seen in calculated and observed ^{77}Se NMR-shifts. Diselenide **6** showed a more than 3-fold higher reactivity than the corresponding des-bromo compound **3a** and ebselen when evaluated in the coupled reductase assay. Experiments followed for longer time (2 h) confirmed that diselenide **6** is a better GPx-catalyst than **11**. On the basis of ^{77}Se-NMR experiments, a catalytic mechanism for diselenide **6** was proposed involving selenol, selenosulfide and seleninic acid intermediates. At low concentration (10 μM) where it showed only minimal toxicity, it could scavenge ROS produced by MNC- and PMNC-cells more efficiently than Trolox.

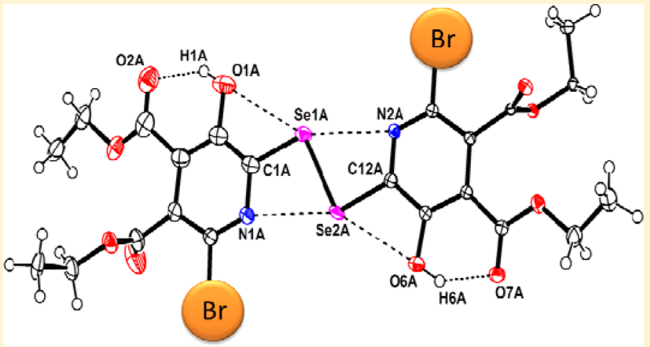

INTRODUCTION

Pyridoxine (**1a**) is a member of the vitamin B6 family of pyridinolic compounds, which serve as cofactors in the metabolism of amino acids.[1] The biologically active form is obtained after phosphorylation of the 5-hydroxymethyl group and oxidation of the remaining alcohol to an aldehyde. The basic structure of the vitamin B6-compounds has been subjected to numerous modifications. The purpose could be to introduce the cofactor into a functioning artificial enzyme,[2] or, with drug applications in mind, to alter the biological activity of the compound.[3] In this respect, the only remaining unsubstituted position 6 in the pyridinol scaffold has been the target for many structural variations. Early on, Korytnyk[4] found that halogens (F, Cl, Br; **1b**−**1d**) in this position caused a change both in the physicochemical (pK_a-values) and biological properties of the compounds. More recently, Jacobson[5] reported on the use of various 6-arylazo-substituted compounds **1e** as potent P2 receptor antagonists. 6-Hydroxymethyl (**1f**), 6-(alkylthio)methyl (**1g**)[6] and 6-trifluoromethyl (**1h**)[7] derivatives were recently prepared for the first time.

Structural modifications of the vitamin B6-scaffold have also been performed with the purpose to impose on the compounds capacities that the parent compound does not show. For example, introduction of a strongly electron donating dimethylamino group in position 6 in pyridoxine (**1i**) or pyridoxamine turned the compounds into excellent radical

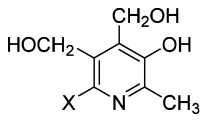

1a X = H; **1f** X = CH_2OH
1b X = F; **1g** X = CH_2SR
1c X = Cl; **1h** X = CF_3
1d X = Br; **1i** X = NMe_2
1e X = N=N-Ar

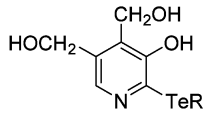

2 R = alkyl

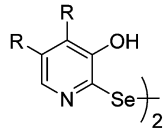

3a R = COOEt
3b R = CH_2OH

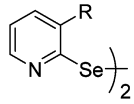

4a R = H
4b R = COOH
4c R = $CONH_2$

Received: April 10, 2015
Published: July 2, 2015

DOI: 10.1021/acs.joc.5b00797
J. Org. Chem. 2015, 80, 7385−7395

Scheme 1. Synthesis of 6-Bromo Substituted Diselenide 6 and Monoselenide 7

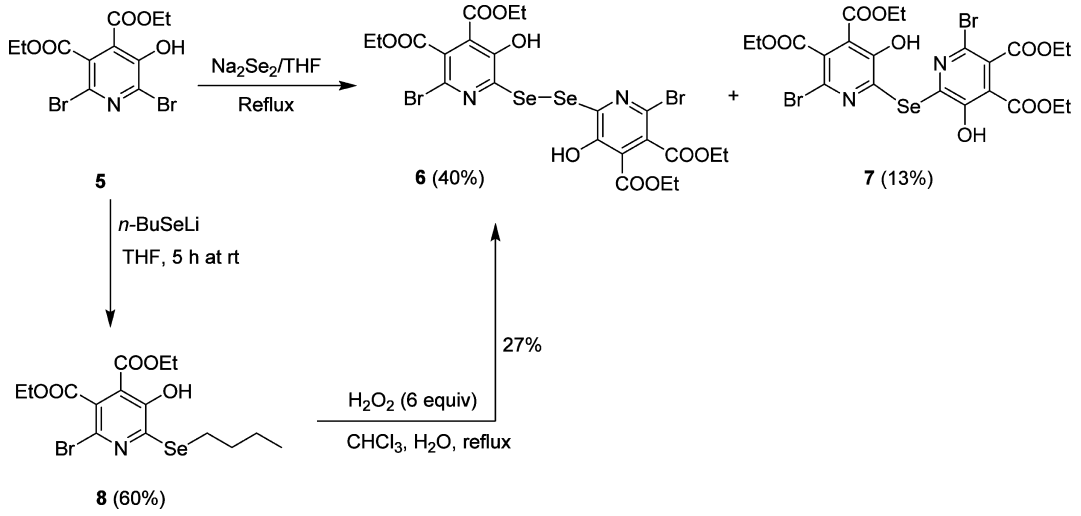

Scheme 2. Synthesis of 6-Bromo Substituted Diselenides 11 and 12

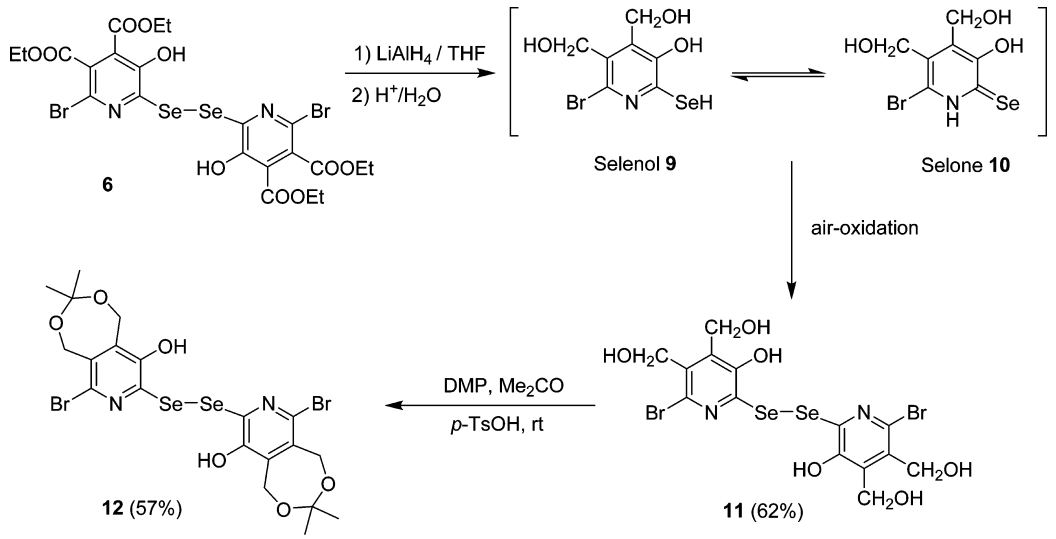

trapping agents[8] that could inhibit the formation of advanced glycation end products (AGEs).[9] In a similar vein, substitution of the 2-methyl group in pyridoxine for an alkyltelluro group (**2**) turned the vitamin into a potent chain-breaking antioxidant that could trap peroxyl radicals some ten times more rapidly than α-tocopherol.[10] As an extension of this work, we recently prepared the pyridoxine-derived diselenides **3a** and **3b**.[11] It was our hope that compounds of this kind could mimic the action of the glutathione peroxidase (GPx) enzymes[12] and act as hydroperoxide decomposing antioxidants. Considerable progress has been made recently in the search for simple organoselenium compounds that could mimic the action of the GPx-enzymes. The list of such compounds include ebselen and analogues,[13] diselenides,[14] selenenate/seleninate esters[15] as well as other selenium containing compounds.[16] As assessed by three different methods, the simplest pyridine-derived diselenide—di-2-pyridyl diselenide (**4a**)—has been reported to act as a fairly active glutathione peroxidase mimic.[11,17,18] Some data are also available concerning the pharmacological properties of this compound.[19] The corresponding nicotinic acid (**4b**)- and nicotinamide (**4c**)-based diselenides were also found to mimic the GPx-enzymes.[20,21] In the latter case, it was proposed (and corroborated by ^{77}Se NMR spectroscopy) that a selone was involved in the mechanism responsible for reduction of hydrogen peroxide. In the case of pyridoxine-derived diselenide **3b**, such a selone was in fact isolable and the structure determined by X-ray crystallography.[11] Diselenides **3b** and **4c** were both 2-fold more active than ebselen when evaluated in the coupled reductase assay. With the perspective to get some more insight into the structural requirements for the high GPx-activity of pyridoxine-derived diselenides and improve the performance of compound **3**, we have introduced bromine into the remaining vacant pyridinolic position 6. As described in the following, this slight variation in the structure has major implications for the reactivity of these compounds.

RESULTS AND DISCUSSION

Synthesis. Our approach to a pyridoxine-derived diselenide carrying a 6-bromo-substituent is based on aromatic nucleophilic substitution (S_NAr). Treatment of the known 2,6-dibromo-4,5-bis(carboethoxy)-3-pyridinol (**5**)[10] with in situ generated Na_2Se_2 under reflux conditions produced the desired diselenide **6** as the major product (Scheme 1). However, the crude product also contained small amounts of another

DOI: 10.1021/acs.joc.5b00797
J. Org. Chem. 2015, 80, 7385−7395

selenium-containing compound, which was inseparable by conventional column chromatography. By careful crystallization of the mixture from diethyl ether it was possible to isolate the red diselenide **6** in 40% yield and the yellow byproduct **7** in 13% yield. The structural assignment of the two products was not trivial. Since the ^{77}Se NMR shifts of compounds **6** and **7** were very similar (450 and 474 ppm, respectively) we initially assigned them both as diselenides differing only in the attachment (2,2′, 2,6′, or 6,6′) of selenium to the two pyridine rings. Finally, the structures of the two compounds were determined by single crystal X-ray analysis (vide infra). This confirmed the structure of **6** as a 2,2′-diselenide and showed that byproduct **7** is in fact the corresponding monoselenide. Obviously, only the 2-bromo substituent in the starting material undergoes S_NAr-substitution even under rather forcing conditions. We speculate that this could be the result of less steric hindrance at position 2 and hydrogen bonding of the nucleophile. The formation of monoselenide is probably due to the presence of Na_2Se, which is formed as a byproduct when sodium is allowed to react with an equimolar amount of elemental selenium. The modest isolated yield of diselenide and the formation of undesired product **7** prompted us to try alternative approaches to **6**. For example, in situ prepared *n*-BuSeLi was found to react with the dibromide to give selenide **8** in 60% yield. However, the following oxidation and selenoxide oxidation returned only small amounts (27%) of diselenide **6**.

The reduction of ester groups in **6** with $LiAlH_4$ was carried out in THF and the reaction mixture worked-up under acidic conditions (Scheme 2). During reduction, the Se−Se bond was also cleaved. After protonation, a selenol **9** or its tautomer, selone **10**, were probably formed initially. However, none of these species were stable in an atmosphere of air and their oxidation product—diselenide **11**—was isolated in 62% yield. This is in contrast to our previous results with a compound lacking the 6-bromo substituent. In case of the des-bromo derivative, the corresponding selone was air-stable and isolable under similar reaction conditions.[11] In order to obtain a less water-soluble compound, the vicinal hydroxymethyl groups in **11** were acetonide protected (compound **12**; 57% yield) at room temperature with 2,2-dimethoxypropane (DMP) in acetone containing an equimolar amount of *p*-toluenesulfonic acid (*p*-TsOH) monohydrate. For reference purposes, 2-bromo-4,5,6-tris(carboethoxy)-3-pyridinol,[10] carrying a carboethoxy group in position 6, was treated with Na_2Se_2 to produce diselenide **13** as a yellow liquid in 45% yield. However, due to high water-solubility, we were unsuccessful in the isolation of the $LiAlH_4$-reduction product of this diselenide.

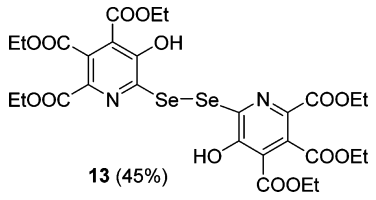

13 (45%)

Crystals of diselenide **6** and selenide **7** suitable for X-ray crystallography were obtained by slow evaporation of MeOH/THF-solutions (1:1) of the compounds at room temperature. The geometry around the Se1A and Se2A atoms in **6** is bent with bond angles of 92.9(6)° and 92.2(5)°, respectively (Figure 1). The two pyridinolic OH groups are intramolecularly hydrogen bonded to the carbonyl oxygens of the neighboring ester groups. The H···O distances (H1A···O2A 1.845 Å, H6A···O7A 1.892 Å) are significantly shorter than the sum of the van der Waals radii of the hydrogen and oxygen atoms (2.72 Å).[22] The most interesting feature of this structure is the four-membered rings formed by weak intramolecular Se···O interactions (Se2A···O6A 2.916 Å, Se1A···O1A 2.912 Å) with pyridinolic oxygen atoms in the same ring and Se···N interactions (Se2A···N1A 2.888 Å, Se1A···N2A 2.922 Å) with nitrogen atoms in the other pyridyl ring. These Se···O and Se···N interactions are significantly shorter than the sum of the van der Waals radii of these two atoms (Se and O atoms = 3.42 Å; Se and N atoms = 3.45 Å). As a result of all these interactions, diselenide **6** adopts an almost planar, "transoid" conformation with a torsion angle C1A-Se1A-Se2A-C12A of −178.08° (Figure 1; lower). This angle is often in the range of 80−90° in other dipyridyl diselenides.[23a,b] The intramolecular interactions and rare torsion angles are similar to those previously reported for bis(3,5-dimethyl-2-pyridyl) diselenide (Se···N 2.901 Å; C−Se−Se−C 180°)[23c] and bis(*N*-phenyl-3-carboxamido-2-pyridyl) diselenide (Se···N 2.887 Å; C−Se−Se−C 180°).[20] Planar structures of diorganyl ditellurides with a dihedral angle of 180° has also been reported.[23d,e] The bent and far from planar structure of selenide **7** is shown in Figure S1 in the Supporting Information.

DFT Calculations. To find out more about the role of the 6-bromo substituent in the pyridoxine-derived diselenides, computational studies were carried out.[24−27] The geometries of diselenides **3a**, **6** and **11** were fully optimized at the B3LYP/6-311+G(d) level of theory (see Table S1−S6 for optimized geometries and coordinates in the Supporting Information). The geometry of diselenide **6** showed good agreement with the X-ray structure. Compound **11** was also essentially planar, but this was not the case with compound **3a**. To estimate the extent of $n_O \rightarrow \sigma^*_{Se-Se}$ and $n_N \rightarrow \sigma^*_{Se-C}$ bonding, the corresponding orbital interactions were studied by performing natural bond orbital (NBO) second-order perturbation analysis. These studies indicated weak Se···O interactions ($E_{Se\cdots O}$ = 1.1 kcal/mol) and Se···N interactions ($E_{Se\cdots N}$ = 2.5 kcal/mol) in compounds **6** and **11** (Table 1). No such interactions were possible in nonplanar compound **3a**. The presence of the electron withdrawing 6-Br substituent was expected to be reflected also in the net atomic charge on selenium. Charges calculated by natural population analysis (NPA) confirmed that the positive charge at selenium is higher in compounds **6** (+0.310) and **11** (+0.294) than in **3a** (+0.174). The effect of the bromo substituent was also seen in calculated as well as experimental ^{77}Se NMR chemical shifts (Table 1). The signals for compounds **6** and **11** were strongly downfield-shifted as compared to those of **3a**.

Furthermore, the topology of the electron density at the Se···N and Se···O bond critical points using Bader's theory of atoms in molecules (AIM) was studied. However, due to the weakness of Se···O interactions, we were unable to identify the bond critical point using the AIM2000 software package (for AIM molecular graphs see Figure S2 in the Supporting Information). However, calculated parameters including electron density ($\rho_{Se\cdots N}$), Laplacian ($\nabla^2\rho_{Se\cdots N}$) and the total electron energy density ($H_{Se\cdots N}$) suggest that there are weak electrostatic interactions between atoms (see Table S7 in the Supporting Information). The introduction of bromine into the vacant pyridinolic positions in compounds **3a** and **3b** had a rather dramatic effect on the structure. We were also curious to see how the halogen substituent would influence the stability of the

DOI: 10.1021/acs.joc.5b00797
J. Org. Chem. 2015, 80, 7385−7395

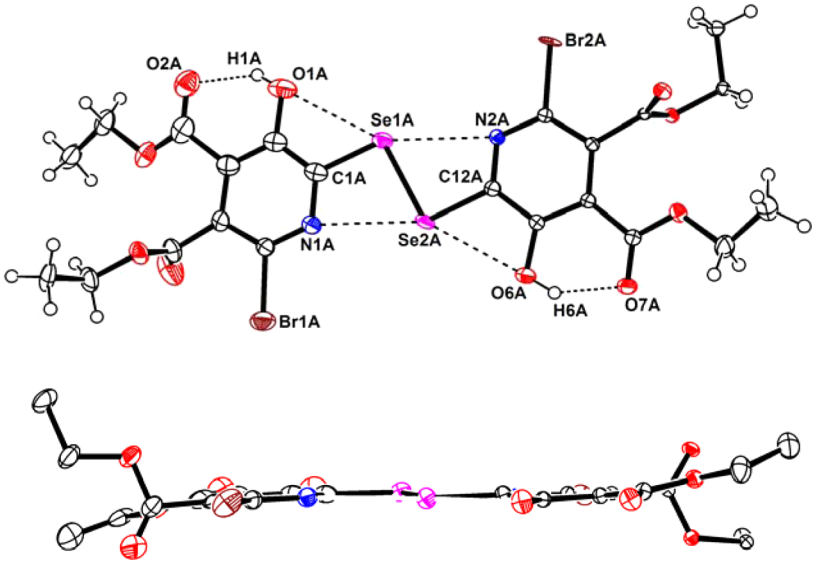

Figure 1. ORTEP diagram (up) top view, (down, H atoms are omitted for clarity) side view of diselenide **6**. Thermal ellipsoids are set at 50% probability. Significant bond lengths [Å] Se1A-C1A 1.910(2), Se2A-C12A 1.919(18), Se1A-Se2A 2.344(2), Se2A···N1A 2.888, Se1A···N2A 2.922, Se2A···O6A 2.916, Se1A···O1A 2.912, H1A···O2A 1.845, H6A···O7A 1.892, and angles [°] O1A···Se1A-Se2A 145.15, O6A···Se2A-Se1A 145.47, C1A-Se1A-Se2A 92.9(6), C12A-Se2A-Se1A 92.2(5), C1A-Se1A-Se2A-C12A −178.08.

Table 1. Second-Order Perturbation Theory of Fock Matrix Using NBO Analysis[a]

					NPA		
compound	$r_{Se\cdots O}$ [Å]	$E_{Se\cdots O}$ (kcal mol^{-1})	$r_{Se\cdots N}$ [Å]	$E_{Se\cdots N}$ (kcal mol^{-1})	q_{Se}	q_{Br}	^{77}Se NMR[b]
6	2.926	1.11	2.991	2.50	+0.310	+0.081	598 (450)
11	2.933	1.11	3.001	2.50	+0.294	+0.044	563 (408)
3a	–	–	–	–	+0.174	–	417 (298)

[a]NPA charges, GIAO ^{77}Se NMR chemical shifts calculated in the gas phase at the B3LYP/6-311+G(d,p) level on the B3LYP/6-31+G(d)-level-optimized geometries. [b]The values are referenced with respect to Me_2Se (δ = 0 ppm). The experimental values are given in parentheses.

tautomeric selenol (**9**) and selone (**10**) forms (Figure 2) which were postulated as intermediates in the transformation of **6** to **11**. The geometries of these species were therefore optimized in the gas phase.

selenol **9** selone **10**

H^{SCF}_{rel} = +3.9 kcal/mol H^{SCF}_{rel} = 0.0 kcal/mol

Figure 2. Calculated energies for selenol and selone tautomers.

Our calculations show that the selone tautomer is more stable than the selenol, but only by 3.9 kcal/mol. In case of the corresponding des-bromo analogues, the (isolable) selone was calculated to be more stable than the selenol by 12.2 kcal/mol. It is therefore not surprising that selone **10** could not be isolated. The calculated bond order (1.37) for the C−Se bond of the selone and the negative NBO charge on Se (−0.19) are indicative of only partial double bond character and contribution from a zwitterionic resonance. AIM analysis of the electron density ($\rho_{Se\cdots N}$ = 0.0247 ea_0^{-3}), the Laplacian of the electron density ($\nabla^2\rho_{Se\cdots H}$ = 0.0525 ea_0^{-5}) and the total energy density at the bond critical point ($H_{Se\cdots H}$ = −0.00098 ea_0^{-4}) in the selone Se···H intramolecular hydrogen bond, suggested both electrostatic and covalent interactions.

Glutathione Peroxidase-like Activity. When incorporated into organic molecules, selenium is easily redox-cycled (easily oxidized and easily reduced). This is the basis for the GPx-like activity of several classes of organoselenium compounds. The catalytic cycle responsible for the hydroperoxide decomposing activity could differ from one catalyst to another, but it often includes more than two species. In the case of diselenide catalysts, functional groups from the following list could be involved: selenol/selenolate, selenenic acid, diselenide, selenosulfide and seleninic acid. Intramolecular secondary Se···N and Se···O-interactions in the catalyst are often important.[28] The role of the N/O substituent could be to increase the reactivity of the catalytically active species by destabilizing them, to sterically protect them from overoxidation or to act as a base to produce a more reactive species. The GPx-like activities of all new pyridoxine compounds were assessed by the coupled reductase assay in an aqueous pH 7.5 phosphate buffer.[14a] In this system (Scheme 3) glutathione reductase (GR) serves to reduce any oxidized glutathione (GSSG) formed by the action of the GPx-catalyst on hydrogen peroxide/GSH using β-nicotinamide adenine dinucleotide phosphate (NADPH) as a cofactor. GPx-activities were conveniently determined as initial rates (ν_0) for the consumption of NADPH as recorded by UV-spectroscopy at 340 nm for the initial 10 s of reaction. Values corrected for the spontaneous reaction of GSH with H_2O_2 (25.1 ± 1.5 μM

DOI: 10.1021/acs.joc.5b00797
J. Org. Chem. 2015, 80, 7385−7395

Scheme 3. Coupled Reductase Assay

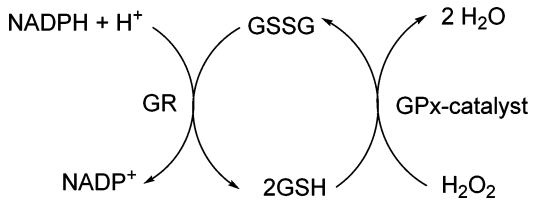

min^{-1}) for compounds prepared are shown in Table 2, panel A. As bench-marks and references, ebselen and **4a** were included. Controls in the absence of both hydrogen peroxide and GSH showed that none of the catalysts studied were substrates for GR (Table 2, panel D). Controls containing GSH, but none of hydrogen peroxide showed considerable initial consumption of NADPH both with ebselen (23.3 μM min^{-1}) and diselenide **6** (84.5 μM min^{-1}) (Table 2, panel C). Presumably, this is because GSSG is formed by reaction of GSH with selenosulfide formed (vide infra). We cannot exclude, though, that the selenosulfide could act as a substrate for GR. This has previously been proposed for GSeSG, the selenosulfide formed from selenoglutathione and glutathione.[14k] Control experiments where GSH had been subtracted from the normal assay (Table 2, panel B) showed some activity for **4a** (16.5 μM min^{-1}) and diselenide **11** (18.7 μM min^{-1}). We hypothesize that this is because the oxidized form of the catalyst (selenenic or seleninic acids) may be a substrate for GR. In the standard assay (Table 2, panel A), bromopyridine-derived diselenides **6** (217.1 μM min^{-1}), **11** (143.1 μM min^{-1}) and **12** (123.4 μM min^{-1}) all showed higher GPx-activity than ebselen (60.5 μM min^{-1}) and **4a** (42.0 μM min^{-1}). It is noteworthy here that diselenide **3a** (71.8 μM min^{-1}), the des-bromo analogue of **6**, is a considerably less active catalyst. Similarly, diselenide **11** was found to be a better catalyst than **3b** (100.1 μM min^{-1})[11] lacking the bromo substituent. Triester catalyst **13** showed only poor GPx-activity. This was also true for monoselenide **7**, which is likely to catalyze hydrogen peroxide decomposition via selenide/selenoxide redox cycling.[29]

All compounds were also evaluated for their capacity to catalyze H_2O_2-oxidation of thiophenol to diphenyl disulfide in methanol (Table 2, panel E).[14b] Initial rates of PhSSPh formation were determined by UV-spectroscopy and corrected for the spontaneous oxidation of PhSH. Whereas catalyst **6** was essentially inactive in this assay, diselenides **11** (ν_0 = 35.8 μM min^{-1}) and **12** (ν_0 = 27.1 μM min^{-1}) performed considerably better than ebselen (ν_0 = 1.3 μM min^{-1}).

Determination of Catalytic Parameters. Detailed kinetic studies were carried out with the two most active catalysts in the coupled reductase assay. To see the effect of the GSH-concentration on catalysis, initial rates of NADPH-consumption (ν_0) at a fixed concentration of H_2O_2 were determined for catalysts **6** and **11**. For both compounds, ν_0 showed a rapid initial increase, followed by saturation kinetics. In a similar fashion, the concentration of H_2O_2 was also varied while the concentration of GSH was kept constant. In this case no saturation was observed at higher (up to 3 mM) concentrations of the oxidant. Lineweaver–Burk plots ($1/\nu_0$ versus the reciprocal of the substrate concentration, 1/[substrate]) were near to linear (see Tables S8–S10 and Figures S3–S10 in the Supporting Information). Catalytic parameters such as the maximum velocity (V_{max}), Michaelis constant (K_M), catalytic constant (k_{cat}) and catalytic efficiency (η) for **6** and **11** are shown in Table 3. The K_M-value for **6** (0.024 mM) is

Table 3. Catalytic Parameters (V_{max}, K_M, k_{cat}, and η) for Catalysts 6 and 11

	V_{max} (μM min^{-1})	K_M (mM)	k_{cat} (min^{-1})	η (mM^{-1} min^{-1})
		catalyst **6**		
GSH (variable)[a]	250.00	0.024	12.50	520.83
H_2O_2 (variable)[b]	833.33	1.97	41.67	21.15
		catalyst **11**		
GSH (variable)[a]	199.60	0.16	9.98	62.37
H_2O_2 (variable)[b]	423.73	1.16	21.19	18.26

[a]Assay conditions: Phosphate buffer (100 mM), pH 7.5, GSH (variable), NADPH (0.2 mM), EDTA (1 mM), GR (1.3 unit mL^{-1}), H_2O_2 (0.80 mM) and catalysts (20 μM). [b]Assay conditions: Phosphate buffer (100 mM), pH 7.5, GSH (1 mM), NADPH (0.2 mM), EDTA (1 mM), GR (1.3 unit mL^{-1}), H_2O_2 (variable) and catalysts (20 μM).

Table 2. GPx-like Activities of Antioxidants As Determined by Initial Rates of NADPH Consumption in the Coupled Reductase Assay and PhSSPh Formation in PhSH Assay

	initial rates for the reduction of H_2O_2, ν_0 (μM min^{-1})				
	A	B	C	D	E
catalysts	with GSH[a]	without GSH[b]	without H_2O_2[c]	with GR[d]	PhSH assay[e]
Ebselen	60.5 ± 1.9	1.3 ± 0.5	23.3 ± 3.3	none	1.3 ± 0.2
4a	42.0 ± 0.5	16.5 ± 2.1	2.4 ± 0.9	0.5 ± 0.1	inactive
3a	71.8 ± 1.2	1.3 ± 0.4	12.2 ± 1.0	2.5 ± 0.8	4.2 ± 0.5
6	217.1 ± 1.6	1.4 ± 0.2	84.5 ± 3.4	1.8 ± 0.5	inactive
7	22.4 ± 1.2	1.8 ± 0.1	1.8 ± 0.6	1.8 ± 0.6	0.5 ± 0.1
11	143.1 ± 1.4	18.7 ± 1.7	14.6 ± 2.1	2.1 ± 0.4	35.8 ± 1.5
12	123.4 ± 1.2	4.1 ± 1.5	8.5 ± 1.2	0.5 ± 0.1	27.1 ± 2.0
13	36.5 ± 0.9	none	3.5 ± 0.8	none	0.8 ± 0.1

[a]Assay conditions: Phosphate buffer (100 mM), pH 7.5 with ethylenediaminetetraacetic acid (EDTA; 1 mM), GSH (1 mM), NADPH (0.2 mM), GR (1.3 unit mL^{-1}), H_2O_2 (0.80 mM) and catalysts (20 μM). [b]The reaction conditions were the same as in *a* but GSH was not added. [c]The reaction conditions were the same as in *a* but H_2O_2 was not added. [d]The reaction conditions were the same as in *a* but H_2O_2 and GSH were not added. Initial rates (ν_0) were corrected for the spontaneous oxidation of GSH (25.1 ± 1.5 μM min^{-1}). [e]PhSH assay conditions: PhSH (1 mM), H_2O_2 (3.75 mM) and catalysts (0.01 mM) in MeOH. Initial reduction rates (ν_0) were corrected for the spontaneous oxidation of PhSH (1.3 ± 0.1 μM min^{-1}). Errors correspond to ± SD for triplicates.

DOI: 10.1021/acs.joc.5b00797
J. Org. Chem. 2015, 80, 7385–7395

significantly lower than recorded for **11** (0.16 mM) and the catalytic efficiency (η) almost 8-fold higher when the GSH concentration is varied. Obviously, diselenide **6** is a better GPx-catalyst than **11**.

Consumption of Hydrogen Peroxide. The action of GPx-mimics **6** and **11** (10 mol %) as catalysts together with GSH, NADPH, GR and H_2O_2 in phosphate buffer was also followed for much longer time (200 min) than the initial phase of reaction. During this period a significant decrease in the absorbance of NADPH was observed (Figure 3). Catalyst **6** was

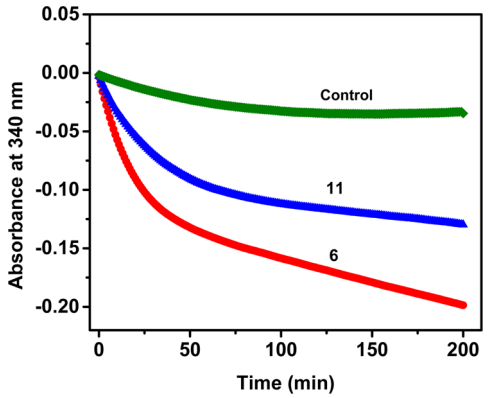

Figure 3. NADPH-consumption with time in the absence (control) and presence of catalysts **6** and **11**. Assay conditions: reactions were carried out with phosphate buffer (100 mM), pH 7.5, with EDTA (1 mM), GSH (0.10 mM), NADPH (0.20 mM), GR (1.3 unit mL^{-1}), H_2O_2 (20 μM) and catalyst (2 μM).

again found superior to **11.** After correction for the spontaneous oxidation of GSH, NADPH-consumption corresponding to complete reduction of all the hydrogen peroxide present in the assay would occur after ca. 50 min. However, as seen from the Figure 3, consumption continues also after this point, but at a slower rate. This could be because selenol formed in the reaction is continuously air-oxidized to diselenide. In line with this proposal, the concentration of NADPH decreased more or less linearly with time over 200 min when hydrogen peroxide was subtracted from the assays containing catalysts **6** and **11** (see Figure S11 in the Supporting Information).

Mechanistic Studies. In order to gain more information about the mechanism responsible for the GPx-activity, ^{77}Se NMR experiments in [D_6]DMSO were carried out with diselenide **6** (δ = 437 ppm). Upon addition of 1 equiv of GSH (dissolved in 200 μL of water), the diselenide peak disappeared completely and a signal at δ = 511 ppm, corresponding to selenosulfide **14**, was observed (Scheme 4). Further addition of 1 equiv of GSH to the mixture did not cause any visible change in the spectra and no peak which could be ascribed to a selenol **15** could be seen. However, indirect evidence for selenol formation could be obtained. When GSH was added to a solution of diselenide **6** and iodobutane, a peak at δ = 342 ppm, corresponding to butyl pyridyl selenide **8**, appeared. When diselenide **6** was allowed to react with a larger excess of GSH, a broad peak at δ = 142 ppm was observed, which is likely to be due to selenol **15**. When 1 equiv of hydrogen peroxide was added to the selenosulfide/selenol-mixture produced from diselenide plus 2 equiv of GSH, diselenide **6** was reformed. A selenenic acid is likely to be a reactive intermediate in this reaction. On further addition of

Scheme 4. Proposed Catalytic Cycle for the Decomposition of H_2O_2 in the Presence of GSH and Catalyst 6

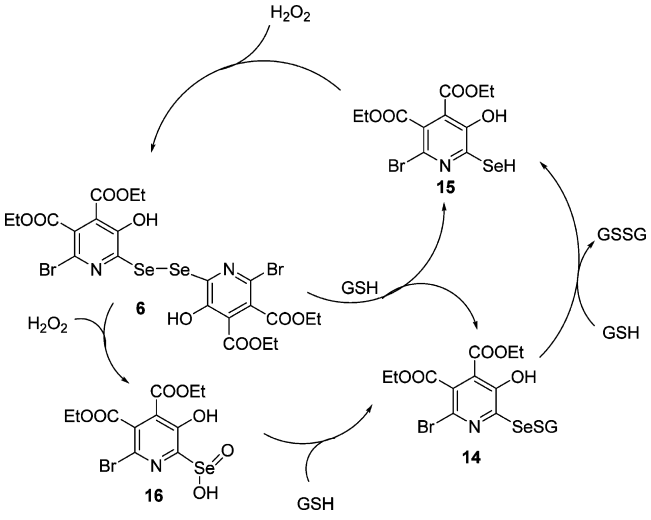

hydrogen peroxide, a peak at δ = 1215 ppm, corresponding to seleninic acid **16**, appeared. After addition of 4 equiv of the oxidant, this was the only peak in the spectrum. Addition of 3 equiv of GSH at this point caused the reappearance of selenosulfide **14**. On the basis of all these experiments, the mechanism for reduction of hydrogen peroxide could be pictured as shown in Scheme 4. The electron-withdrawing ester and bromine substituents serve to improve the leaving group properties of the pyridylseleno moiety. This would facilitate selenol formation via nucleophilic attack of GSH on selenium in diselenide **6** and on sulfur in selenosulfide **14**. Our experiments described above indicate that substitution is more facile in the former case. In the absence of hydrogen peroxide, O_2-oxidation of the selenol and subsequent reactions of the diselenide and selenosulfide with GSH would produce GSSG and therefore cause NADPH-consumption (vide supra).

To find an explanation for the poor performance of diselenide **6** in the thiophenol assay, some ^{77}Se NMR experiments were performed. For solubility reasons, deutero-chloroform was used as a solvent instead of methanol. Even after addition of several equivalents of thiophenol to diselenide **6**, we did not see any peak corresponding to a selenosulfide. Apparently, thiophenol is such a poor nucleophile that the diselenide is left untouched. However, upon further addition of H_2O_2 to the mixture a signal at δ = 609 ppm appeared, which is likely to be due to selenosulfide **17**. Probably, the diselenide is oxidized to a seleninic acid which is then reduced by thiol present. However, upon further addition of hydrogen peroxide (up to 20 equiv) the seleninic acid was never reformed. Further addition of thiophenol (up to 40 equiv; see the Supporting Information for ^{77}Se NMR spectra) to the above mixture, also did not cause any change in the ^{77}Se NMR spectrum. It therefore seems that the selenosulfide is a dead end in the catalytic cycle.

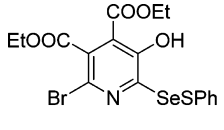

17

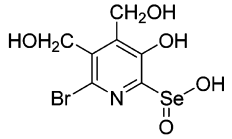

18

DOI: 10.1021/acs.joc.5b00797
J. Org. Chem. 2015, 80, 7385−7395

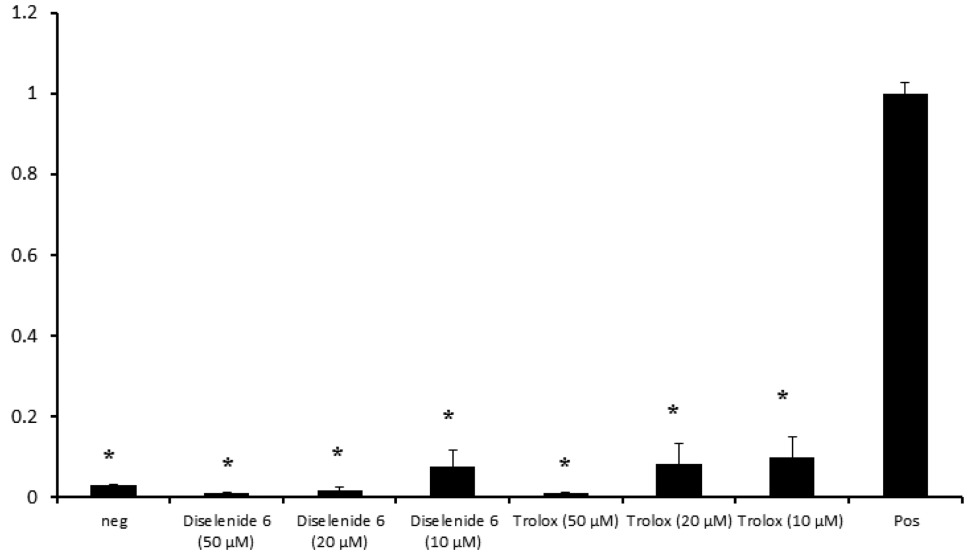

Figure 4. Chemiluminescence (normalized to positive control) from PMA-stimulated MNC-cells exposed to various concentrations (10, 20, and 50 μM) of diselenide **6** and Trolox. * Indicates $p < 0.05$ compared to positive control. $N = 3$ to 6 for each group from 4 independent experiments.

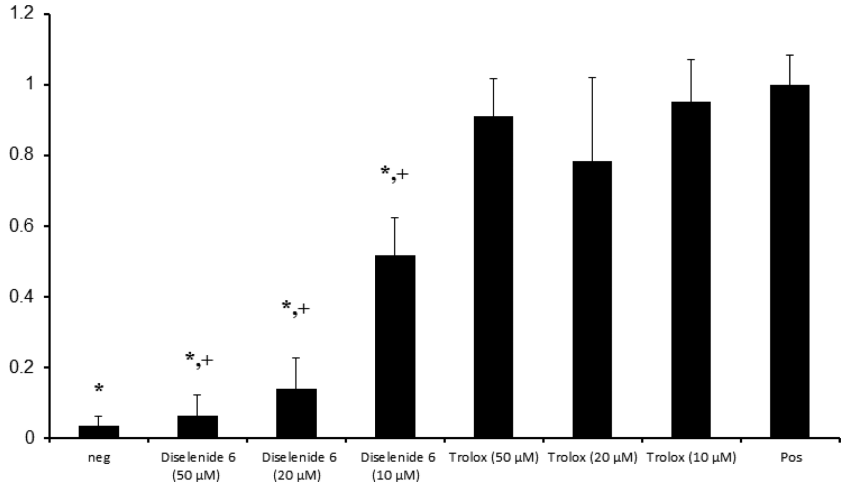

Figure 5. Chemiluminescence (normalized to positive control) from PMNC-cells exposed to various concentrations (10, 20, and 50 μM) of diselenide **6** and Trolox. * and + indicates $p < 0.05$ compared to positive control and Trolox of same concentration, respectively (e.g., diselenide **6** at 50 μM compared to Trolox 50 μM). $N = 6$ to 10 for each group from 5 independent experiments.

Diselenide **11** upon oxidation produced a seleninic acid **18** (δ = 1217 ppm). When thiophenol was added in excess to the mixture, a new signal at δ = 204 ppm appeared in the ^{77}Se NMR spectrum. This is likely to be due to selone **10** (the corresponding, isolable des-bromo selone resonated at δ = 137 ppm[11] and the additional bromine is likely to cause a downfield shift). Therefore, under the conditions of the thiophenol assay, the GPx-activity of compound **11** can be explained by a catalytic cycle involving diselenide, seleninic acid and selone intermediates. A similar mechanism is also likely to be operative with diselenide **12** (see the Supporting Information).

ROS-Scavenging Capacity of Diselenide 6. An overproduction of reactive oxygen-(ROS) and reactive nitrogen species (RNS) such as superoxide, hydrogen peroxide and peroxynitrite is characteristic to pathologies such as inflammation, atherosclerosis and stroke. We were curious to see if diselenide **6** had a scavenging effect on these reactive species in a more biological setting. The total ROS (extra- and intracellular) from phorbol myristate acetate (PMA)-stimulated freshly isolated human mononuclear cells (MNC; Figure 4) and polymorphonuclear cells (PMNC; Figure 5) were therefore measured in the presence of diselenide **6** by luminol enhanced chemiluminescence (CL). As can be seen, diselenide **6** scavenges ROS in a dose-dependent manner at least as good (MNC) or better (PMNC) than Trolox, which was used as a reference antioxidant.

In contrast, the corresponding des-bromo diselenide **3a** caused only a slight (25%) reduction in the total chemiluminescence at the highest concentration (50 μM) tried (data not shown).

Cell Viability/Proliferation. In order to assess the toxicity of diselenide **6**, MC3T3 (a preosteoblast cell line) and HEK293T (an embryonic kidney cell line) cells were exposed to the concentrations of diselenide **6** and Trolox that effectively reduced ROS generation from PMNC/MNC cells (Figure 6). Whereas at 10 and 20 μM concentrations no toxic effects upon either of the cell lines were observed over 6 days, some reduction in cell viability was seen with diselenide **6** at 50 μM.

DOI: 10.1021/acs.joc.5b00797
J. Org. Chem. 2015, 80, 7385−7395

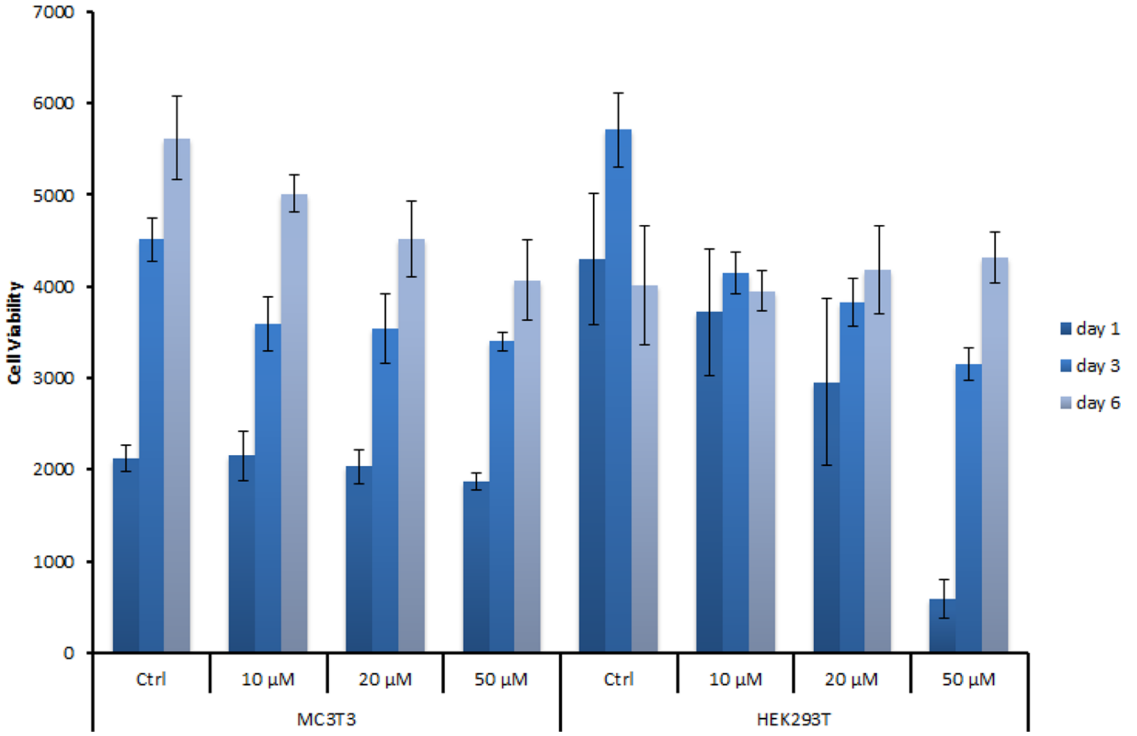

Figure 6. Relative cell viability of MC3T3 and HEK293T cells in the presence of 10, 20, and 50 μM concentrations of diselenide **6** as determined by Alamar Blue measurements after 1, 3, and 6 days.

CONCLUSIONS

Some time ago we prepared the pyridoxine-like diselenides **3a** and **3b** and examined their glutathione peroxidase-like properties. It was our hope that these vitamin B6 look-a-likes would be better tolerated in biological sytems than other diselenide-based GPx-mimics. Unless we had made some unexpected observations, this would probably be the end of the story. The peculiar finding we did is concerned with compounds **6** and **11**, carrying an extra bromine in position 6. In contrast to what was seen with **3a**/**3b**, the GPx-activity of the tetraester **6** was much higher than recorded for tetraol **11**. Overall, **6** was the best catalyst with a 3-fold higher activity than ebselen. We also confirmed that the improved antioxidant effect translated into a more biologically relevant system. Compound **6** was an excellent quencher of ROS produced in PMA-stimulated MNC- and PMNC-cells as revealed by chemiluminescence studies. Obviously the small perturbation in the molecule (bromine instead of hydrogen) has major implications for structure and reactivity. The extra halogen would add to the electron-withdrawing effect of the two ester groups in the pyridyl moiety and make selenium even more positive. This is compensated for by weak intramolecular coordination of the chalcogen to pyridinolic HO- and N-groups, resulting in an almost planar, conformation of the molecule in the crystal. Reactivity-wise, the bromine turns the pyridylseleno group into a better leaving group. Nucleophilic attack of thiol (GSH) on selenium in diselenide **6** and on sulfur in selenosulfide **14** is therefore greatly facilitated. This is likely to be the key to understanding the high GPx-activity of **6** as compared to **3a**, **3b** and **11**. It remains to be seen how the novel diselenide will be received when introduced into biological systems. We have shown that its toxicity is insignificant at concentrations where it could efficiently inhibit ROS-production in stimulated leucocytes. It would therefore seem worthwhile to test it for treatment of diseases where the natural antioxidant systems are overwhelmed (inflammation, stroke, cardiovascular diseases etc.).

EXPERIMENTAL SECTION

^{1}H and ^{13}C NMR spectra for all new compounds were recorded on 300 MHz (^{1}H: 300 MHz; ^{13}C: 75 MHz) and 400 MHz (^{1}H: 399.97 MHz; ^{13}C: 100.58 MHz) spectrometers, using the residual solvent peaks of $CDCl_3$ (^{1}H δ 7.26; ^{13}C δ 77.2), and [D_6]DMSO (^{1}H δ 2.50; ^{13}C δ 39.5), as an indirect reference to TMS (δ = 0 ppm). ^{77}Se NMR spectra were recorded on a 400 MHz (^{77}Se: 76 MHz) instrument using Ph_2Se_2 as an internal standard (δ = 460 ppm relative to Me_2Se δ = 0 ppm). Flash column chromatography was performed using silica gel (0.04−0.06 mm). Melting points were uncorrected. High resolution mass spectra (HRMS) were obtained using a time-of-flight (TOF) instrument equipped with electrospray ionization (ESI) and operating in the positive ion mode. Tetrahydrofuran (THF) was dried in a solvent purification system by passing it through an activated alumina column before use.

Di-[6-bromo-4,5-bis(carboethoxy)-3-hydroxy-2-pyridyl] Diselenide (6). Compound **5**[10] (1.17 g, 2.94 mmol) in dry THF (5 mL) was added to a brown stirring suspension of in situ prepared (from sodium and selenium[30]) Na_2Se_2 (5.88 mmol) in dry THF (25 mL) under nitrogen atmosphere at 0 °C. The flask was allowed to warm to room temperature and then heated at reflux for 24 h. Water (50 mL) was added to the mixture and stirring continued for an additional 10 min. The content of the flask was then neutralized with hydrochloric acid (2 M aq.) and the aqueous layer that separated was extracted with $CHCl_3$ (3 × 20 mL). The combined organic layers were dried over anhydrous Na_2SO_4 and evaporated. Purification of the residue by column chromatography on silica gel using 30% ethyl acetate/pentane as eluent afforded a difficult to separate mixture of two compounds. Recrystallization from diethyl ether afforded compound **6** (450 mg, 40%) as a red solid and **7** (140 mg, 13%) as a yellow solid.

Diselenide **6**: mp 132−135 °C; ^{1}H NMR ($CDCl_3$) δ 1.36−1.42 (several peaks, 12H), 4.38 (q, J = 7.2 Hz, 4H), 4.44 (q, J = 7.2 Hz, 4H), 11.15 (s, 2H); ^{13}C NMR ($CDCl_3$) δ 13.9, 14.1, 62.5, 63.9, 116.0,

DOI: 10.1021/acs.joc.5b00797
J. Org. Chem. 2015, 80, 7385−7395

127.7, 128.9, 146.3, 153.3, 165.3, 166.9; ^{77}Se NMR ($CDCl_3$) δ 450; ^{77}Se NMR ([D_6]DMSO) δ 437; HRMS (TOF MS ES$^+$) m/z calcd for $C_{22}H_{22}Br_2N_2O_{10}Se_2$ [M + H]$^+$ 792.8050, found 792.8047.

Diselenide **6** was also obtained by heating of selenide **8** (125 mg, 0.280 mmol) with H_2O_2 (6 equiv of a 35% aq. solution), H_2O (0.50 mL) and $CHCl_3$ (2 mL) at reflux for 16 h at 80 °C. Purification by column chromatography as above afforded diselenide **6** (30 mg, 27%).

Di-[6-bromo-4,5-bis(carboethoxy)-3-hydroxy-2-pyridyl] Selenide (7). mp 151−154 °C; ^{1}H NMR ($CDCl_3$) δ 1.38−1.44 (several peaks, 12H), 4.38 (m, 8H), 11.21 (s, 2H); ^{13}C NMR ($CDCl_3$) δ 13.9, 14.1, 62.6, 64.0, 116.1, 127.0, 129.7, 145.9, 154.8, 165.3, 167.1; ^{77}Se NMR ($CDCl_3$) δ 474; HRMS (TOF MS ES$^+$) m/z calcd for $C_{22}H_{22}Br_2N_2O_{10}Se$ [M + H]$^+$ 712.8885, found 712.8873.

Butyl 6-Bromo-4,5-bis(carboethoxy)-3-hydroxy-2-pyridyl Selenide (8). Compound **5** (397 mg, 1.00 mmol) was added to a solution of *n*-BuSeLi prepared in situ from Se powder (180 mg, 2.00 mmol) and *n*-BuLi (1.6 M, 1.25 mL, 2.00 mmol) in dry THF (25 mL) at 0 °C under an inert atmosphere. The reaction was allowed to warm to room temperature and then stirred for 5 h. The solvent was removed under reduced pressure and the residue dissolved in $CHCl_3$ and washed with water. The organic layer and the $CHCl_3$ extracts of the aqueous layer were combined and dried over anhydrous Na_2SO_4. After evaporation and column chromatography using 10% ethyl acetate/pentane as eluent, the pure title compound **8** was isolated as a yellow liquid (270 mg, 60%): ^{1}H NMR ($CDCl_3$) δ 0.94 (t, J = 7.4 Hz, 3H), 1.36−1.49 (several peaks, 8H), 1.76 (quintet, J = 7.1 Hz, 2H), 3.19 (t, J = 7.4 Hz, 2H), 4.37−4.45 (several peaks, 4H), 11.19 (s, 1H); ^{13}C NMR ($CDCl_3$) δ 13.8, 13.9, 14.1, 23.2, 25.2, 31.9, 62.4, 63.7, 113.8, 125.9, 127.4, 151.6, 153.6, 165.9, 167.5; ^{77}Se NMR ($CDCl_3$) δ 342; HRMS (TOF MS ES$^+$) m/z calcd for $C_{15}H_{20}BrNO_5Se$ [M + H]$^+$ 453.9768, found 453.9782.

Di-[6-bromo-3-hydroxy-bis(4,5-hydroxymethyl)-2-pyridyl] Diselenide (11). A solution of diselenide **6** (200 mg, 0.250 mmol) in THF (5 mL) was added dropwise to a stirred suspension of $LiAlH_4$ (58 mg, 1.51 mmol) in dry THF (10 mL) under an inert atmosphere at 0 °C. The reaction mixture was then stirred at room temperature for overnight and H_2SO_4 (10% aq.) was added to quench the excess $LiAlH_4$. After 5 min the mixture was neutralized with NaOH (5% aq.) and the separated aqueous layer extracted several times with ethyl acetate. The combined organic extracts were dried over anhydrous Na_2SO_4 and evaporated to yield the title compound **11** as a yellow solid (98 mg, 62%): mp >250 °C; ^{1}H NMR ([D_6]DMSO) δ 4.60 (s, 4H), 4.76 (s, 4H), 10.38 (br s, 2H); ^{13}C NMR ([D_6]DMSO) δ 56.2, 59.6, 133.4, 134.6, 136.6, 141.4, 150.1; ^{77}Se NMR ([D_6]DMSO) δ 408; HRMS (TOF MS ES$^+$) m/z calcd for $C_{14}H_{14}Br_2N_2O_6Se_2$ [M + H]$^+$ 624.7627, found 624.7629.

Di-[6-bromo-3,3-dimethyl-9-hydroxy-[1,3]dioxepino[5,6-*c*]-pyridine-8-yl] Diselenide (12). 2,2-Dimethoxypropane (0.5 mL) and *p*-toluenesulfonic acid monohydrate (21 mg, 0.11 mmol) were added to a stirred solution of diselenide **11** (70 mg, 0.11 mmol) in acetone (5 mL), and stirring was continued for an additional 3 h at room temperature. During this period the solution turned redish. The mixture was then poured into a saturated aqueous solution of $NaHCO_3$. The aqueous layer was extracted with $CHCl_3$ and dried over anhydrous Na_2SO_4. Removal of the solvent under vacuo and purification of the residue by silica gel column chromatography using 40% ethyl acetate/pentane as eluent afforded the title compound **12** as a yellow solid (45 mg, 57%): mp 198−201 (dec.) °C; ^{1}H NMR ($CDCl_3$) δ 1.50 (s, 12H), 4.91 (s, 4H), 4.95 (s, 4H); ^{13}C NMR ($CDCl_3$) δ 23.8, 59.5, 63.8, 102.8, 130.1, 137.1, 139.2, 150.5 (one peak is missing/overlapping); ^{77}Se NMR ([D_6]DMSO) δ 413; HRMS (TOF MS ES$^+$) m/z calcd for $C_{20}H_{22}Br_2N_2O_6Se_2$ [M + H]$^+$ 704.8253, found 704.8260.

Di-[4,5,6-tris(carboethoxy)-3-hydroxy-2-pyridyl] Diselenide (13). 2-Bromo-4,5,6-tris(carboethoxy)-3-pyridinol[10] (0.900 g, 2.30 mmol) dissolved in dry THF (5 mL) was added dropwise to a brown suspension of in situ prepared Na_2Se_2 (4.60 mmol) in dry THF (20 mL) under nitrogen atmosphere at 0 °C. The reaction was allowed to warm to room temperature and then stirred for 10 h. Water (50 mL) was added to the reaction mixture and stirring continued for 10 min. The mixture was then neutralized with hydrochloric acid (2 M aq.) and the aqueous layer that separated was extracted with ethyl acetate (3 × 20 mL). The combined organic layers were dried over anhydrous Na_2SO_4 and evaporated. Purification of the residue by column chromatography on silica gel using 50% ethyl acetate/pentane as eluent afforded the title compound as a yellow liquid (400 mg, 45%): ^{1}H NMR ($CDCl_3$) δ 1.25−1.44 (several peaks, 18H), 4.25−4.50 (several peaks, 12H), 11.91 (br s, 2H); ^{13}C NMR ($CDCl_3$) δ 13.8, 13.9, 14.1, 62.0, 62.2, 63.9, 115.2, 130.3, 136.4, 146.3, 157.6, 163.4, 165.7, 167.8; ^{77}Se NMR ($CDCl_3$) δ 483; HRMS (TOF MS ES$^+$) m/z calcd for $C_{28}H_{32}N_2O_{14}Se_2$ [M + H]$^+$ 781.0262, found 781.0245.

Coupled Reductase Assay. The GPx-like activities of novel organoselenium compounds were determined by UV-spectroscopy following the protocol of Wilson with slight modifications.[14a] The test mixture contained GSH (1 mM), ethylene- diaminetetraacetic acid (EDTA, 1 mM), glutathione reductase (GR, 1.3 unit mL^{-1}), and β-nicotinamide adenine dinucleotide phosphate (NADPH, 0.20 mM) in potassium phosphate buffer (100 mM, pH 7.5) and catalyst (20 μM) was initiated by addition of H_2O_2 (0.80 mM) at 21 °C. Initial reaction rates were based on the consumption of NADPH as assessed by UV-spectroscopy at 340 nm. The initial reaction rates were determined in triplicate and calculated during the initial 10 s of reaction by using 6.22 mM^{-1} cm^{-1} as the extinction coefficient for NADPH. GPx-data reported in Table 2 are means ± SD.

PhSH Assay. The GPx-like activities of organoselenium compounds were determined in MeOH by UV-spectroscopy following Tomoda's protocol with slight modifications.[14b] The test mixture contained PhSH (1 mM) and catalyst (0.01 mM) at 21 °C and the reaction was initiated by addition of H_2O_2 (3.75 mM). The formation of diphenyl disulfide (Ph_2S_2) during the first 10 s of reaction as assessed by UV-spectroscopy at 305 nm was used as a measure of initial reaction rate, using 1.24 mM^{-1} cm^{-1} as the extinction coefficient for Ph_2S_2. GPx-data reported in Table 2 are means ± SD for triplicates.

Biological Studies. Blood buffy coats obtained from anonymous blood donors from Uppsala University hospital were diluted in a 1:1 ratio with 1× phosphate buffered saline (PBS, Fischer Scientific MA) and mononuclear cells were segregated using Ficoll-Paque (Fischer Scientific) plus density gradient centrifugation. Briefly, the diluted blood was gently placed on top of Ficoll-Paque and then centrifuged at 400*g* (MSE, UK) between 20 and 30 min. After removing the plasma layer, the mononuclear (MNC) layer was collected, washed with PBS, and then spun at 100*g* for 15 min. This washing procedure was repeated for a total of 3 times. Total cell number was counted using a hemocytometer and trypan blue exclusion method (Life Technologies CA). To isolate polymorphonuclear cells (PMNC), the blood buffy coat was processed using Ficoll-Paque centrifugation as described above. The blood pellet was then suspended in 3%dextran/0.9% saline for 20 min. The supernatant was then collected and the cell pellet collected after centrifugation at 250*g* for 10 min. To remove erythrocyte, the pellet was subjected to 0.2% saline solution for 20 s and then an equal volume of 1.6% saline was added. Then the cells were spun at 250*g* for 10 min and the pellet was suspended in PBS. For counting PMNC using a hemocytometer, cells dilutions were prepared using a 1:1 dilution in 6% acetic acid in order to distinguish polymorphonuclear cells from mononuclear cells.

Chemiluminescence Assay. To measure release of reactive oxygen species (ROS) from monocytes and neutrophils, a luminol amplified chemiluminescence assay was conducted. All measurements were performed in white 96 well plates (PerkinElmer, MA) at 37 °C in 1× PBS with 50 mM of luminol (Sigma-Aldrich, MO), 0.1 M NaOH (Sigma), 2 μg/mL of horse radish peroxidase (Fischer-Scientific), different concentrations of diselenide **6** and Trolox (Sigma) initially diluted in DMSO (Serva, Germany). Approximately, 2 × 10^5 cells were plated in each well and then stimulated to generate ROS using 500 nM of 1 μM phorbol myristate acetate (PMA, Sigma). Luminescence readings were taken using a multiplate reader (Infinite M200 Tecan, Switzerland) every 2 min for 2 h. Total ROS was quantified by determining the area under the chemiluminescence kinetic curve. Experiments were repeated at 4−5 times with n = 3 per group per experiment. For statistical analysis, ANOVA was performed

DOI: 10.1021/acs.joc.5b00797
J. Org. Chem. 2015, 80, 7385−7395

in IBM SPSS software with Scheffe posthoc tests. *P* values below 0.05 were considered significant.

Cell Proliferation and Toxicity Assay. MC3T3 and HEK293T (plating density: 5×10^3 and 20×10^3 per well respectively in a 96 well plate) were let adhered after plating for 24 h in α-MEM (Gibco, CA) supplemented with 10% FBS (Gibco) and 1% pen/strep (Gibco). Then the cells were exposed to different concentrations of diselenide **6** (50, 20, and 10 μM) for 24 h, washed and then fed with fresh α-MEM every other day. To assess cell viability, AlamarBlue assay was conducted (Invitrogen, CA) on day 1, 3, and 6 after treatment with diselenide **6**. Briefly, cells were washed with 1× PBS and then incubated with AlamarBlue (1:20 dilution in phenol red free α-MEM (Gibco)) for 1.5 h and then fluorescence was read with a plate reader (Infinite M200) at 560 nm excitation and 590 nm emissions. Experiments were repeated twice with $n = 6$ for each group.

X-ray Crystallographic Analysis. X-ray crystallographic studies for obtaining the structures of compounds **6** and **7** were carried out on a Bruker Apex 2 using graphite-monochromatized Mo Kα radiation (λ = 0.7107 Å).[31] The structures were solved by direct methods (SHELXS-2013) and refined by a full-matrix least-squares procedure on F^2 for all reflections using SHELXL-2013 software.[32] Hydrogen atoms were localized by geometrical means. A riding model was chosen for refinement. The isotropic thermal parameters of hydrogen atoms were fixed at 1.5 times and 1.2 times U(eq) of the corresponding carbon atoms for sp^3 C−H and sp^2 C−H bonds, respectively. Crystallographic data for the structures reported in this paper have been deposited with the Cambridge Crystallographic Data Centre (CCDC) as supplementary publications. CCDC 1032632 (for compound **6**), and CCDC 1032633 (for compound **7**) contain the supplementary crystallographic data for this paper. These data can be obtained free of charge from the Cambridge Crystallographic Data Centre via www.ccdc.cam.ac.uk/data_request/cif.

Computational Details. All theoretical calculations were executed by using Gaussian 09 suite of quantum chemical programs.[33] The hybrid Becke 3-Lee−Yang−Parr (B3LYP) exchange correlation functional was implemented for density functional theory (DFT) calculations.[34] The geometry optimizations were carried out at the B3LYP level of DFT by using the 6-311+G(d) basis sets. The quantifications of orbital interaction were done by natural bond orbital (NBO) analysis at B3LYP/6-311+G(d,p) level.[35] The ^{77}Se NMR calculations were performed at B3LYP/6-311+G (d,p) level on B3LYP/6-311+G(d)-level-optimized geometries by using the gauge-including atomic orbital (GIAO) method (referenced with respect to the peak of Me_2Se).[36] Atoms in molecules (AIM)[37−39] calculations have also been used to confirm distinct bond critical point between the two interacting atoms.

■ ASSOCIATED CONTENT

Supporting Information

^{1}H, ^{13}C and ^{77}Se NMR data for all new compounds prepared. Results from kinetic studies of compounds prepared (maximum velocities, Lineweaver−Burk plots, control experiments in the absence of hydrogen peroxide for long-time). X-ray crystal structure of compound **7**. Some details of the refinement have been listed in Table S12. Coordinates of optimized geometries. CIF-files for compounds **6** and **7** are also available. The Supporting Information is available free of charge on the ACS Publications website at DOI: 10.1021/acs.joc.5b00797.

■ AUTHOR INFORMATION

Corresponding Authors

*E-mail: vijaypalchem@gmail.com.
*E-mail: lars.engman@kemi.uu.se.

Notes

The authors declare no competing financial interest.

■ ACKNOWLEDGMENTS

The Swedish Research Council and Carl Tryggers Stiftelse för Vetenskaplig Forskning (CTS 13:120 and 13:346) are gratefully acknowledged for financial support. Part of this work was facilitated by the BioMat facility/Science for Life Laboratory at Uppsala University. The authors wish to acknowledge the assistance of Dr. Matthias Zeller and Youngstown State University for the collection of X-ray data. The X-ray diffractometer was funded by NSF Grant CHE 0087210, Ohio Board of Regents Grant CAP-491, and by Youngstown State University (for datasets starting with "Apex") and NSF Grant DMR 1337296 (for datasets starting with "Quest" or "Prosp").

■ REFERENCES

(1) Combs, G. F., Jr. *The Vitamins: Fundamental Aspects in Nutrition and Health*, 4th ed.; Elsevier: Amsterdam, 2012.
(2) (a) Murakami, Y.; Kikuchi, J.; Hisaeda, Y.; Hayashida, O. *Chem. Rev.* **1996**, *96*, 721−758. (b) Liu, L.; Breslow, R. *Bioorg. Med. Chem.* **2004**, *12*, 3277−3287.
(3) (a) Korytnyk, W.; Srivastava, S. C.; Angelino, N.; Potti, P. G. G.; Paul, B. *J. Med. Chem.* **1973**, *16*, 1096−1101. (b) Korytnyk, W.; Angelino, N. *J. Med. Chem.* **1977**, *20*, 745−749. (c) Pham, V.; Zhang, W.; Chen, V.; Whitney, T.; Yao, J.; Froese, D.; Friesen, A. D.; Diakur, J. M.; Haque, W. *J. Med. Chem.* **2003**, *46*, 3680−3687.
(4) Korytnyk, W.; Srivastava, S. C. *J. Med. Chem.* **1973**, *16*, 638−642.
(5) (a) Kim, Y.-C.; Brown, S. G.; Harden, T. K.; Boyer, J. L.; Dubyak, G.; King, B. F.; Burnstock, G.; Jacobson, K. A. *J. Med. Chem.* **2001**, *44*, 340−349. (b) Kim, Y.-C.; Lee, J.-S.; Sak, K.; Marteau, F.; Mamedova, L.; Boeynaems, J.-M.; Jacobson, K. A. *Biochem. Pharmacol.* **2005**, *70*, 266−274.
(6) Shtyrlin, N. V.; Pavelyev, R. S.; Pugachev, M. V.; Sysoeva, L. P.; Musin, R. Z.; Shtyrlin, Y. G. *Tetrahedron Lett.* **2012**, *53*, 3967−3970.
(7) Yu, J.-X.; Cui, W.; Bourke, V. A.; Mason, R. P. *J. Med. Chem.* **2012**, *55*, 6814−6821.
(8) Culbertson, S. M.; Enright, G. D.; Ingold, K. U. *Org. Lett.* **2003**, *5*, 2659−2662.
(9) Culbertson, S. M.; Vassilenko, E. I.; Morrison, L. D.; Ingold, K. U. *J. Biol. Chem.* **2003**, *278*, 38384−38394.
(10) Singh, V. P.; Poon, J.; Engman, L. *J. Org. Chem.* **2013**, *78*, 1478−1487.
(11) Singh, V. P.; Poon, J.; Butcher, R. J.; Engman, L. *Chem. - Eur. J.* **2014**, *20*, 12563−12571.
(12) Hatfield, D. L.; Berry, M. J.; Gladyshev, V. N., Eds.; *Selenium: Its Molecular Biology and Role in Human Health*, 3rd ed.; Springer-Verlag: New York, 2012.
(13) (a) Parnham, M. J.; Biedermann, J.; Bittner, Ch.; Dereu, N.; Leyck, S.; Wetzig, H. *Agents Actions* **1989**, *27*, 306−308. (b) Dakova, B.; Lamberts, L.; Evers, M.; Dereu, N. *Electrochim. Acta* **1991**, *36*, 631−637. (c) Back, T. G.; Dyck, B. P. *J. Am. Chem. Soc.* **1997**, *119*, 2079−2083. (d) Bhabak, K. P.; Mugesh, G. *Chem. - Eur. J.* **2007**, *13*, 4594−4601. (e) Satheeshkumar, K.; Mugesh, G. *Chem. - Eur. J.* **2011**, *17*, 4849−4857. (f) Selvakumar, K.; Shah, P.; Singh, H. B.; Butcher, R. J. *Chem. - Eur. J.* **2011**, *17*, 12741−12755. (g) Singh, V. P.; Singh, H. B.; Butcher, R. J. *Eur. J. Org. Chem.* **2011**, *2011*, 5485−5497. (h) Balkrishna, S. J.; Kumar, S.; Azad, G. K.; Bhakuni, B. S.; Panini, P.; Ahalawat, N.; Tomar, R. S.; Detty, M. R.; Kumar, S. *Org. Biomol. Chem.* **2014**, *12*, 1215−1219. (i) Pacula, A. J.; Scianowski, J.; Aleksandrzak, K. B. *RSC Adv.* **2014**, *4*, 48959−48962.
(14) (a) Wilson, S. R.; Zucker, P. A.; Huang, R. C.; Spector, A. *J. Am. Chem. Soc.* **1989**, *111*, 5936−5939. (b) Iwaoka, M.; Tomoda, S. *J. Am. Chem. Soc.* **1994**, *116*, 2557−2561. (c) Mugesh, G.; Panda, A.; Singh, H. B.; Punekar, N. S.; Butcher, R. J. *J. Am. Chem. Soc.* **2001**, *123*, 839−850. (d) Zhang, X.; Xu, H.; Dong, Z.; Wang, Y.; Liu, J.; Shen, J. *J. Am. Chem. Soc.* **2004**, *126*, 10556−10557. (e) Tripathi, S. K.; Patel, U.; Roy, D.; Sunoj, R. B.; Singh, H. B.; Wolmershäuser, G.; Butcher, R. J. *J. Org. Chem.* **2005**, *70*, 9237−9247. (f) Lv, S.-W.; Wang, X.; Mu, Y.;

DOI: 10.1021/acs.joc.5b00797
J. Org. Chem. 2015, 80, 7385−7395

Zang, T.; Ji, Y.; Liu, J.; Shen, J.; Lou, G. *FEBS J.* **2007**, *274*, 3846−3854. (g) Bhabak, K. P.; Mugesh, G. *Chem. - Eur. J.* **2008**, *14*, 8640−8651. (h) Bhabak, K. P.; Mugesh, G. *Chem. - Eur. J.* **2009**, *15*, 9846−9854. (i) Alberto, E. E.; Soares, L. C.; Sudati, J. H.; Borges, A. C. A.; Rocha, J. B. T. *Eur. J. Org. Chem.* **2009**, *2009*, 4211−4214. (j) Singh, B. G.; Bag, P. P.; Kumakura, F.; Iwaoka, M.; Priyadarsini, K. I. *Bull. Chem. Soc. Jpn.* **2010**, *83*, 703−708. (k) Yoshida, S.; Kumakura, F.; Komatsu, I.; Arai, K.; Onuma, Y.; Hojo, H.; Singh, B. G.; Priyadarsini, K. I.; Iwaoka, M. *Angew. Chem., Int. Ed.* **2011**, *50*, 2125−2128. (l) Press, D. J.; Back, T. G. *Org. Lett.* **2011**, *13*, 4104−4107. (m) Tripathi, S. K.; Sharma, S.; Singh, H. B.; Butcher, R. J. *Org. Biomol. Chem.* **2011**, *9*, 581−587.

(15) (a) Back, T. G.; Moussa, Z. *J. Am. Chem. Soc.* **2003**, *125*, 13455−13460. (b) Zade, S. S.; Singh, H. B.; Butcher, R. J. *Angew. Chem., Int. Ed.* **2004**, *43*, 4513−4515. (c) Singh, V. P.; Singh, H. B.; Butcher, R. J. *Chem. - Asian J.* **2011**, *6*, 1431−1442. (d) Press, D. J.; McNeil, N. M. R.; Hambrook, M.; Back, T. G. *J. Org. Chem.* **2014**, *79*, 9394−9401.

(16) (a) Kuzma, D.; Parvez, M.; Back, T. G. *Org. Biomol. Chem.* **2007**, *5*, 3213−3217. (b) Press, D. J.; Mercier, E. A.; Kuzma, D.; Back, T. G. *J. Org. Chem.* **2008**, *73*, 4252−4255. (c) Yu, S.-C.; Borchert, A.; Kuhn, H.; Ivanov, I. *Chem. - Eur. J.* **2008**, *14*, 7066−7071. (d) Sarma, B. K.; Manna, D.; Minoura, M.; Mugesh, G. *J. Am. Chem. Soc.* **2010**, *132*, 5364−5374. (e) Nascimento, V.; Alberto, E. E.; Tondo, D. W.; Dambrowski, D.; Detty, M. R.; Nome, F.; Braga, A. L. *J. Am. Chem. Soc.* **2012**, *134*, 138−141. (f) Rakesh, P.; Singh, H. B.; Jasinski, J. P.; Golen, J. A. *Dalton Trans.* **2014**, *43*, 9431−9437.

(17) Collins, C. A.; Fry, F. H.; Holme, A. L.; Yiakouvaki, A.; Al-Qenaei, A.; Pourzand, C.; Jacob, C. *Org. Biomol. Chem.* **2005**, *3*, 1541−1546.

(18) Hodage, A. S.; Prabhu, C. P.; Phadnis, P. P.; Wadawale, A.; Priyadarsini, K. I.; Jain, V. K. *J. Organomet. Chem.* **2012**, *720*, 19−25.

(19) Luchese, C.; Brandão, R.; Acker, C. I.; Nogueira, C. W. *Mol. Cell. Biochem.* **2012**, *367*, 153−163 and references cited therein. .

(20) Prabhu, C. P.; Phadnis, P. P.; Wadawale, A.; Priyadarsini, K. I.; Jain, V. K. *J. Organomet. Chem.* **2012**, *713*, 42−50.

(21) Prabhu, P.; Singh, B. G.; Noguchi, M.; Phadnis, P. P.; Jain, V. K.; Iwaoka, M.; Priyadarsini, K. I. *Org. Biomol. Chem.* **2014**, *12*, 2404−2412.

(22) Bondi, A. *J. Phys. Chem.* **1964**, *68*, 441−445.

(23) (a) Kienitz, C. O.; Thöne, C.; Jones, P. G. *Inorg. Chem.* **1996**, *35*, 3990−3997. (b) Bhasin, K. K.; Singh, J. *J. Organomet. Chem.* **2002**, *658*, 71−76. (c) Dhau, J. S.; Singh, A.; Dhir, R. *J. Organomet. Chem.* **2011**, *696*, 2008−2013. (d) Niyomura, O.; Kato, S.; Inagaki, S. *J. Am. Chem. Soc.* **2000**, *122*, 2132−2133. (e) Chauhan, R. J.; Kedarnath, G.; Wadawale, A.; Slawin, A. M. Z.; Jain, V. K. *Dalton Trans.* **2013**, *42*, 259−269.

(24) Iwaoka, M.; Tomoda, S. *J. Am. Chem. Soc.* **1996**, *118*, 8077−8084.

(25) Iwaoka, M.; Komatsu, H.; Katsuda, T.; Tomoda, S. *J. Am. Chem. Soc.* **2004**, *126*, 5309−5317.

(26) Roy, D.; Sunoj, R. B. *J. Phys. Chem. A* **2006**, *110*, 5942−5947.

(27) Sarma, B. K.; Mugesh, G. *ChemPhysChem* **2009**, *10*, 3013−3020.

(28) Mukherjee, A. J.; Zade, S. S.; Singh, H. B.; Sunoj, R. B. *Chem. Rev.* **2010**, *110*, 4357−4416.

(29) Kumakura, F.; Mishra, B.; Priyadarsini, K. I.; Iwaoka, M. *Eur. J. Org. Chem.* **2010**, *2010*, 440−445.

(30) Thompson, D. P.; Boudjouk, P. *J. Org. Chem.* **1988**, *53*, 2109−2112.

(31) *APEX2*; Bruker AXS Inc.: Madison, WI, 2005.

(32) Sheldrick, G. M. *Acta Crystallogr., Sect. A: Found. Crystallogr.* **2008**, *A64*, 112−122.

(33) Frisch, M. J.; Trucks, G. W.; Schlegel, H. B.; Scuseria, G. E.; Robb, M. A.; Cheeseman, J. R.; Scalmani, G.; Barone, V.; Mennucci, B.; Petersson, G. A.; Nakatsuji, H.; Caricato, M.; Li, X.; Hratchian, H. P.; Izmaylov, A. F.; Bloino, J.; Zheng, G.; Sonnenberg, J. L.; Hada, M.; Ehara, M.; Toyota, K.; Fukuda, R.; Hasegawa, J.; Ishida, M.; Nakajima, T.; Honda, Y.; Kitao, O.; Nakai, H.; Vreven, T.; Montgomery, J. A.; Peralta, J. E., Jr.; Ogliaro, F.; Bearpark, M.; Heyd, J. J.; Brothers, E.; Kudin, K. N.; Staroverov, V. N.; Keith, T.; Kobayashi, R.; Normand, J.; Raghavachari, K.; Rendell, A.; Burant, J. C.; Iyengar, S. S.; Tomasi, J.; Cossi, M.; Rega, N.; Millam, J. M.; Klene, M.; Knox, J. E.; Cross, J. B.; Bakken, V.; Adamo, C.; Jaramillo, J.; Gomperts, R.; Stratmann, R. E.; Yazyev, O.; Austin, A. J.; Cammi, R.; Pomelli, C.; Ochterski, J. W.; Martin, R. L.; Morokuma, K.; Zakrzewski, V. G.; Voth, G. A.; Salvador, P.; Dannenberg, J. J.; Dapprich, S.; Daniels, A. D.; Farkas, O.; Foresman, J. B.; Ortiz, J. V.; Cioslowski, J.; Fox, D. J. *Gaussian 09*, Revision c.01/d.01; Gaussian, Inc.: Wallingford, CT, 2010/2013.

(34) (a) Lee, C.; Yang, W.; Parr, R. G. *Phys. Rev. B: Condens. Matter Mater. Phys.* **1988**, *37*, 785−789. (b) Becke, A. D. *J. Chem. Phys.* **1993**, *98*, 5648−5652.

(35) (a) Reed, A. E.; Curtiss, L. A.; Weinhold, F. *Chem. Rev.* **1988**, *88*, 899−926. (b) Glendening, E. D.; Reed, J. E.; Carpenter, J. E.; Weinhold, F. *Natural Bond Orbital (NBO)*, program 3.1; Madison, WI, 1988.

(36) Bayse, C. A. *Inorg. Chem.* **2004**, *43*, 1208−1210.

(37) Bader, R. W. F. *Atoms in Molecules: A Quantum Theory*; Oxford University Press: New York, 1990.

(38) Popelier, P. *Atoms In Molecules: An Introduction*; Pearson: Harlow, 2000.

(39) Beigler-Konig, F.; Schonbohm, J.; Bayles, D. *J. Comput. Chem.* **2001**, *22*, 545−559.

DOI: 10.1021/acs.joc.5b00797
J. Org. Chem. 2015, 80, 7385−7395